Reconstructing Holocene regional subsidence in the Netherlands, utilizing interpolated coastal plain water table rise

K. de Wit[1], R. S. W. van de Wal[1,2], K. M. Cohen[1]

1 Department of Physical Geography, Utrecht University, The Netherlands
2 Institute for Marine and Atmospheric research Utrecht, Utrecht University, The Netherlands

Keywords: Subsidence, glacio-isostatic adjustment (GIA), relative sea-level rise (RSLR), basal peat data

k.dewit@uu.nl

Abstract

Land subsidence is of major concern to coastal plains and deltas, especially when both shallow soft soil subsidence (alteration of Holocene strata) and deeper natural subsidence (including tectonic tectono-sedimentary basin loading and sinking and glacio-isostatic adjustment (GIA)) occur simultaneously, as is the case in the Netherlands. Separation of deeper subsidence components, such as GIA vs. basin tectonics in the total subsidence signal can be difficult, since they often act on similar spatial scales and similar rates. The aim of this study is to improve the estimation and separation of the spatio-temporal GIA component within the total subsidence signal across the Netherlands using a data based approach. Our main observational data for this is a database of all relevant geological paleo-water level index points (e.g. basal peats) in the Dutch coastal plain. Interpolation of this data in a spatio-temporal grid, calculates continuous coastal plain water table maps per time slice and relative groundwater level (GWL) rise curves for any location in the Dutch coastal plain. The spatial parameters in the interpolation formulae and derivates of the interpolation outputs are used to identify and analyse subsidence-induced regional patterns in the relative sea-level rise controlled subareas. Further processing of the results and comparison with alternative interpolation runs (e.g. input undone from components attributable to basin-tectonics), complement the analysis. The ability to produce data-driven, spatially causal break downs of continuous deeper subsidence across the full coastal plain, with the spatial and Holocene-temporal variance quantified as well, is the main result of the current research.

Introduction

Land subsidence is a major societal problem affecting deltas and coastal plains all over the world (Syvitski et al., 2009; Brown & Nicholls, 2015; Minderhoud et al., 2020). Currently, relative sea-level rise (RSLR) is increasing in many coastal areas due to the combined effects of accelerating sea-level rise and exacerbated land subsidence (Oppenheimer et al, 2019). In the Netherlands, both shallow soft soil subsidence and deeper subsidence components are in play, the latter including glacio-isostatic adjustment (GIA) and tectono-sedimentary basin loading and sinking (e.g. Kooi et al., 1998; Fokker et al., 2018). It is difficult to directly measure the current rate-contributions of individual deeper subsidence components, because they are due to slower operating, long term processes, with rates an order of magnitude smaller than that of shallow subsidence (e.g. peat and clay compaction and peat oxidation) (Van de Plassche, 1982; Koster et al., 2018). Additionally, GIA and tectonic subsidence

rates appear to be of the same order of magnitude and regional scale in the western and northern Netherlands, but with different orientations.

Figure 1 (panels a and b) illustrates the subsidence bullseyes that are generally regarded to differ between the basin and GIA components. The magnitudes and exact locations of the basin and GIA bullseyes are not precisely known, and so far have mostly been studied separately, because different methods are used to reconstruct them. Basin sinking under depocenter loading, for example, has been reconstructed with a tectono-sedimentary back-stripping analysis that uses the thickness of the Quaternary and Neogene sequence below the North Sea floor to determine vertical land motion as averaged over the last 2.6 Myr (Kooi et al., 1998; Cohen et al., 2022). The GIA contribution since the last glacial maximum (LGM) in the North Sea area is often assessed using numerically coarse output from large-scale geophysical models. This has used Holocene geological observational sea level index point data (so-called SLIPs) to verify the outcomes of these models at selected sites (e.g. Vink et al., 2007). However, multiple combinations of GIA input result in fairly equal data fits and notable differences in predicted current rates (e.g. reviews in Vermeersen et al., 2018). In other words, the rates and locations of the respective bullseyes and the relative importance of basin and GIA components, and how this spatially varies in the coastal plain and over time are not well known.

The aim of this study is to use a data-based approach to reconstruct the contribution of GIA and basin tectonics to regional subsidence in the Netherlands during the Holocene using coastal plain water level indicators. We perform an analysis of paleo-sea-level and other coastal plain paleo-water level geological data, by means of a spatial-temporal interpolation method that reconstructs Holocene RSLR in four dimensions (X-, Y-, Z- and Time). We use the parameterization of the interpolation trend to identify regional trends in RSLR, and we use kriging of the residuals to resolve sub-regional patterns in the RSLR.

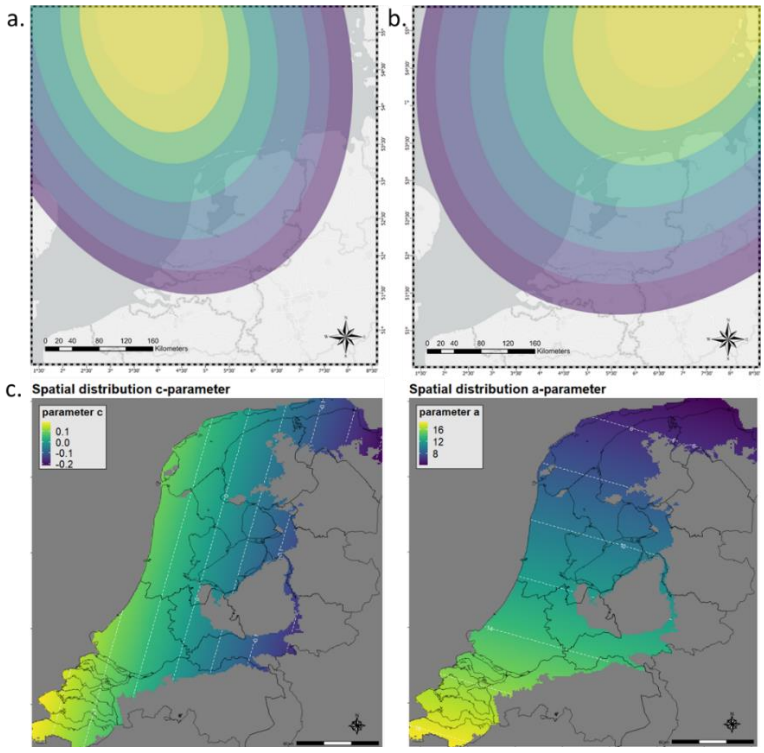

Figure 1 Upper panels: Simplified visualization indicating the expected general orientations of subsidence components attributable to a.) the tectono-sedimentary subsidence of the North Sea basin and b.) glacio-isostatic adjustment in the periphery of the former Scandinavian ice mass. Lower panels the c.) example of the spatial distribution of the c-parameter and a-parameter specified in the interpolation formulae.

Methods

We apply a 3D KT-kriging interpolation method to our dataset (Kriging residuals after applying a Trend function (Eq.1)), performed over the X,Y and T domain. The interpolation predicts GW-table elevations (Z) for given locations of X and Y (study area in Fig. 2; currently at 1x1 km resolution) and for a discrete moment in time, T (from 10 ka to 1 ka, with timesteps of 200 years; Cohen, 2005; Koster et al., 2017). The trend function step of the KT-kriging procedure predicts Z in a normalized form (Z_n) as shown in Eq. 1. Zn is the position between a lower (Z_n=0) and an upper (Z_n=1) bounding envelope surface that were independently reconstructed for both 10 ka and 1 ka (Cohen, 2005). The parameters $c_{(x,y)}$ and $a_{(x,y)}$ in the trend function (Eq. 1) are spatially dependent and optimized by non-linear least squares regression analysis on the observations (the GWL data, 576 observations of X,Y,T and Z (Figure 2), taken from many sea-level and inland water table reconstruction studies, notably: Jelgersma, 1961; Van de Plassche, 1982; Kiden, 1995; Cohen, 2005; Koster et al., 2017; Meijles et al., 2018; Hijma & Cohen, 2019). The inputs $q_{(x,y)}$ and $p_{(t)}$ are prescribed: they are the normalized thickness of the Holocene wedge and the moment in time normalized between 10 ka ($p_{(t)}$ = 0) and 1 ka ($p_{(t)}$ = 1).

$$Z_n = \left(1 - c_{(x,y)}\right)\left(1 - e^{-a_{(x,y)} q_{(x,y)} p_{(t)}{}^{b}}\right) + \left(c_{(x,y)} * p_{(t)}\right) \; (Equation\ 1)$$

After the trend function step (estimation of parameters $a_{(x,y)}$, b, and $c_{(x,y)}$), Z_n results are transformed back to absolute GW-table elevations (Z). At all observation locations residuals (observed – trend) are calculated as input for the kriging step of the KT-kriging procedure. The latter uses ordinary block kriging interpolation (blocks of 1x1 km and 200 years). The combined interpolation output (trend + kriging) thus contains an observations-derived (i) spatially continuous parameterization of trend function parameters and 3D-gridded output (Z_{trend}), and (ii) subregional correction for subregional GWL variation not captured by the overall fitted trend ($Z_{kriging}$). This output is produced independently of GIA modelling which enables cross-comparison.

The KT-kriging method includes spatial variance (interpolation uncertainty, accuracy) outputs. From the trend step, the total standard deviation of the interpolation GWL fields is c. 1.1 m (= trend fitting performance). Close to datapoints, the kriging step lowers this to a block-averaged nugget value of c. 0.2 m (= limitation of basal peat as geological water table reconstruction). The spatial parameters $c_{(x,y)}$ and $a_{(x,y)}$ trend-fitted solutions are used to identify and analyze subsidence-induced regional patterns (Figure 1). Doing this for interpolation runs on different subsets (north-northwest-west-southwest; seaward-inland), helps to understand method input sensitivity, as well as the spatial differences in timing and tempo of relative GWL rise throughout the coastal plain.

Parameter $c_{(x,y)}$ in equation 1 determines the contributions of the non-linear ('sigmoid') and linear term describing Z_n, while parameter $a_{(x,y)}$ (and b) influence the sigmoid shape of the normalized GWL rise curve (more sigmoid when a is high). In a run as in Figure 1c, this means that in inland areas where parameter $a_{(x,y)}$ is low, the relative GWL rises slower and linear, and in seaward areas where it is high it is more sigmoid. Taking in the pattern of $c_{(x,y)}$ as well, this allows to split the trend-function predicted total GWL rise in a Holocene-constant 'linear' part and Holocene-variable 'non-linear' part (decelerating from onset Middle Holocene, 9-8 ka onwards).

Post-processed derivatives of the interpolation outputs are further used to identify and analyse subsidence-induced regional patterns. This processing includes 4D filtering the results to constrain analysis to areas where local GWL variability is mainly mean sea-level rise attributable (not too far inland, not too early in the Holocene when areas were not yet lagoonal-inundated). This feeds an analysis of regional variation and allows to attribute variations in thickness of the Holocene sedimentary wedge to intrinsic topographic (e.g. valleys visible in depth to Top Pleistocene, Figure 2)

and differential subsidence causes (Figure 1), besides contrasting the temporal variation in GWL rise between areas.

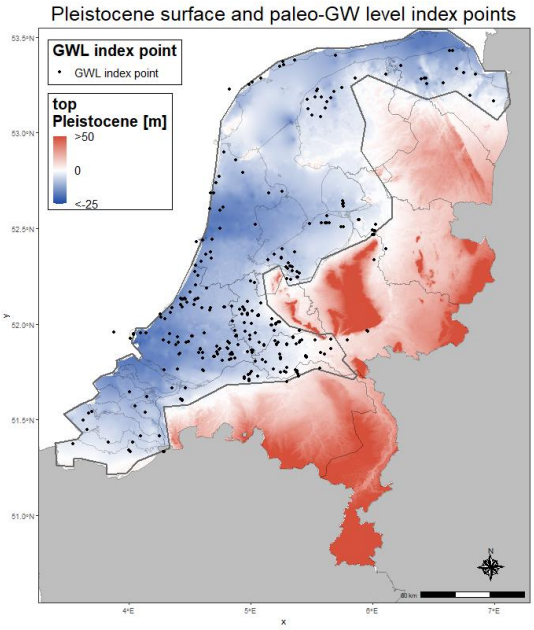

Figure 2 Distribution of geological observations on Holocene GWL index points locations used for this study. The study area is marked with a grey polygon. Depth to base coastal plain is indicated in blue (top Pleistocene, 0 = 0 m NAP ≈ present MSL).

Holocene coastal plain water table rise results

The 4D interpolation output has a flexible hypercube structure, easing the visualization of the data in different forms, such as predicted GWL maps shown (Figure 3 shows four slices, the hypercube stores output every 200 yr). Figure 3 shows that at 8 ka BP the GWL was still very low throughout the coastal plain, with most of the GWL close to the topographic surface of the time (compare patterns in Top Pleistocene in Fig. 2) that features several valleys inherited from the Last Glacial. Note that in the inland direction, the water table rises modestly to grade with Pleistocene surface and feeding river valleys. From 8 ka onwards the GWL starts to rise and topographic gradients in the west and north flatten as the coastal plain establishes over the buried valleys. At 6 ka BP the GWL has risen some 10 meters, subtly more in the North than in the Southwest. Surfaces of that age are encountered c. 2 m lower in the north compared to the southwest. At 4 ka BP, subtle regional differences in GWL are apparent (South to North: meter scale regional variations between Rhine delta, central lagoon and Wadden Sea fringe). The panel for 2 ka BP shows the flattest coastal plain water table reconstruction, just above but close in elevation to that of 4 ka.

The interpolation approach works well for simulating Holocene GWL fields, especially in the previous studied areas at the west coast of the Netherlands. However, work is still ongoing on optimizing the parameterization of the trend function especially in the northern part of the Netherlands, where the GWL index point density is lower (Figure 2). Further development of output visualization (masking, uncertainty) is also foreseen.

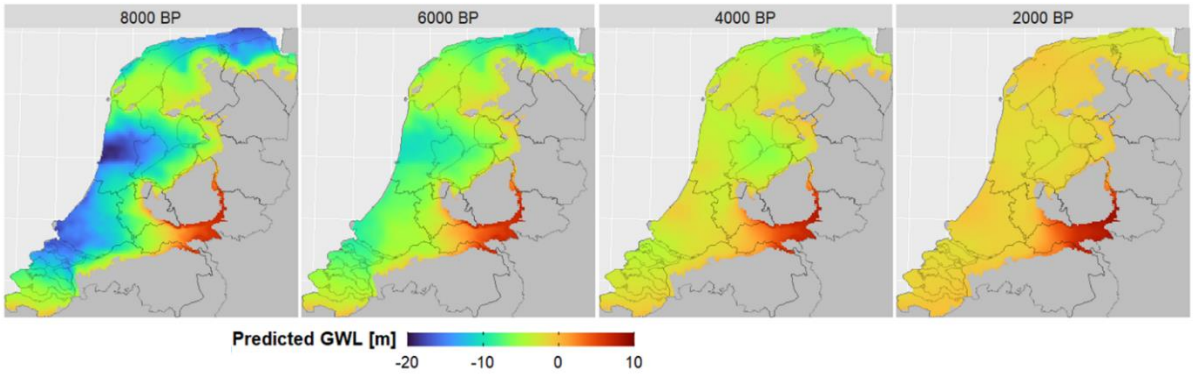

Figure 3 Holocene relative groundwater levels for selected moments as predicted by our 3D KT block kriging procedure.

Preliminary subsidence analysis and discussion

Figure 3 shows that 8 ka, 6 ka and 4 ka 'Middle Holocene' coastal water tables in the Netherlands are geologically encountered deeper in the North than in the South. This implies a different pacing of relative GWL rise in the north, and a greater contribution of subsidence in the relative rise signal in these regions. Presuming that the non-subsidence part of GWL rise in these areas was similar (at least near the modern coast, driven by post-glacial sea level rise), and noting that the basal peat input data is essentially unaffected by shallow soft soil subsidence, Figure 3 and the output of the interpolation in general thus hold a quantification of large scale differential subsidence due to deeper processes, i.e. GIA and basin subsidence (Fig. 1ab). Of these, tectonic subsidence is assumed to be nearly constant during the Holocene, with differences in subsidence rates up to 0.2 m/kyr in the Netherlands, subsidence increasing in a north-west direction (Kooi et al., 1998; Cohen et al., 2022). In contrast, GIA subsidence is expected to decrease from 'Middle' (8-4 ka) to 'Late' Holocene (last 4 ka) times (Vink et al., 2007; Steffen & Wu, 2011). The parameter fitting, the differential subsidence results in Fig. 3, and independent observations (e.g. GPS, tide gauges and InSAR data – beyond the scope of this abstract) suggest that this is quantifiable from the interpolation output.

Stronger GIA-lowering of the north and northeast relative to the southwest can explain part of the differential subsidence observed for the Middle Holocene. In the Late Holocene and modern situation, preliminary interpolation results and comparison with values in literature indicates that 'constant' basin subsidence is of similar magnitude as the decreased GIA signal, at least in the northwest. Also, in the Late Holocene (last 4 ka) the differential subsidence due to deeper subsidence processes is less pronounced and overprinted by other signals, such as soft soil subsidence or seepage. As the parameter fitting steps of our method are sensitive to observational data distribution, it is still difficult to fully determine the relative contributions of GIA and tectonic subsidence to the relative greater subsidence in the North, and quantify the uncertainty. In future work we will run interpolation experiments with GWL index point depths that are corrected for independently estimated basin subsidence rates (source material cited earlier), to isolate the GIA component. Furthermore, a closer cross-comparison between the data-based interpolation outcome and the physics-based GIA models will help further disentangle the GIA and tectonic subsidence signals within the Netherlands.

Conclusion

This study presents a 3D Holocene relative GWL interpolation for the Netherlands, that incorporates regional trends in relative GWL rise, and the output embeds spatio-temporally variant signals of regional scale differential subsidence processes attributable to GIA (Scandinavia peripheral) and basin subsidence (North Sea Basin). The data-driven methodology for analysing background differential

subsidence across the Netherlands, runs independently from physical GIA modelling, allowing for a cross-comparison with such results in the near future.

The current results are nationwide, spatially-continuous coastal plain water table reconstructions through Holocene time. Differential subsidence is particularly visible in the Middle Holocene (8-4 ka) and more subtle in the Late Holocene (last 4 ka). The north of the Netherlands subsided faster than the southwest of the Netherlands, notably in the Middle Holocene when the GIA signal was strong. The north continues to sink relatively faster in the Late Holocene, but the contribution of GIA versus basin subsidence appears to have become of equal size, especially in the northwest of the country. Further work to disentangle the GIA and tectonic subsidence signals within the Netherlands and quantify uncertainty in their attribution are ongoing.

Author contributions

KW, KMC and RSW designed the research. All authors contributed to the writing of the article.

Competing interests

The authors declare that they have no conflict of interest.

Financial report

The research presented in this paper is part of the project Living on soft soils: subsidence and society (grantnr.: NWA.1160.18.259): PhD project WP1.3 - 2020-2024. This project is funded by the Dutch Research Council (NWO-NWA-ORC), Utrecht University, Wageningen University, Delft University of Technology, Ministry of Infrastructure & Water Management, Ministry of the Interior & Kingdom Relations, Deltares, Wageningen Environmental Research, TNO-Geological Survey of The Netherlands, STOWA, Water Authority: Hoogheemraadschap de Stichtse Rijnlanden, Water Authority: Drents Overijsselse Delta, Province of Utrecht, Province of Zuid-Holland, Municipality of Gouda, Platform Soft Soil, Sweco, Tauw BV, NAM.

References

Brown, S., & Nicholls, R. (2015). Subsidence and human influences in mega deltas: the case of the Ganges–Brahmaputra–Meghna. *Science of the Total Environment, 527*, 362-374.

Cohen, K. M. (2005). 3D geostatistical interpolation and geological interpretation of paleo–groundwater rise in the Holocene Coastal Prism in the Netherlands.

Cohen, K. M., Cartelle, V., Barnett, R., Busschers, F. S., & Barlow, N. L. (2022). Last Interglacial sea-level data points from Northwest Europe. *Earth System Science Data*, *14*(6), 2895-2937.

Hijma, M. P., & Cohen, K. M. (2019). Holocene sea-level database for the Rhine-Meuse Delta, The Netherlands: implications for the pre-8.2 ka sea-level jump. QSR.

Jelgersma, S. (1961). Holocene sea-level changes in the Netherlands. *Ph. D. dissertation, Leiden Univ.*

Kiden, P. (1995). Holocene relative sea-level change and crustal movement in the southwestern Netherlands. *Marine Geology*, *124*(1-4), 21-41.

Kooi, H., Johnston, P., Lambeck, K., Smither, C., & Molendijk, R. (1998). Geological causes of recent (~ 100 yr) vertical land movement in the Netherlands. *Tectonophysics*, *299*(4), 297-316.

Koster, K., Stafleu, J., & Cohen, K. M. (2017, Dec). Generic 3D interpolation of Holocene base-level rise and provision of accommodation space, developed for the Netherlands coastal plain and infilled palaeovalleys. *Basin Research, 29*(6), 775-797.

Koster, K., Cohen, K. M., Stafleu, J., and Stouthamer, E.: Using ^{14}C-dated peat beds for reconstructing subsidence by compression in the Holland coastal plain of the Netherlands, J. Coastal Res., 34, 1035–1045, 2018.

Meijles, E. W., Kiden, P., Streurman, H.-J., van der Plicht, J., Vos, P. C., Gehrels, W. R., & Kopp, R. E. (2018). Holocene relative mean sea-level changes in the Wadden Sea area, northern Netherlands. *Journal of Quaternary Science, 33*(8), 905-923.

Minderhoud, P., Middelkoop, H., Erkens, G., & Stouthamer, E. (2020). Groundwater extraction may drown mega-delta: projections of extraction-induced subsidence and elevation of the Mekong delta for the 21st century. *Environmental Research Communications, 2*(1), 011005.

Oppenheimer, M., B.C. Glavovic, J. Hinkel, R. van de Wal, A.K. Magnan, A. Abd-Elgawad, R. Cai, M. Cifuentes-Jara, R.M. DeConto, T. Ghosh, J. Hay, F. Isla, B. Marzeion, B. Meyssignac and Z. Sebesvari (2019). Sea Level Rise and Implications for Low-Lying Islands, Coasts and Communities. IPCC Special Report on the Ocean and Cryosphere in a Changing Climate. Intergovernmental Panel on Climate Change.

Van de Plassche, O. (1982). Sea-level change and water-level movements in the Netherlands during the Holocene. *Ph. D. dissertation, Vrije Universiteit Amsterdam*.

Steffen, H., & Wu, P. (2011). Glacial isostatic adjustment in Fennoscandia—a review of data and modeling. *Journal of geodynamics, 52*(3-4), 169-204.

Syvitski, J. P., Kettner, A. J., Overeem, I., Hutton, E. W., Hannon, M. T., Brakenridge, G. R., Day, J., Vörösmarty, C., Saito, Y., & Giosan, L. (2009). Sinking deltas due to human activities. *Nature Geoscience, 2*(10), 681-686.

Vink, A., Steffen, H., Reinhardt, L., & Kaufmann, G. (2007). Holocene relative sea-level change, isostatic subsidence and the radial viscosity structure of the mantle of northwest Europe (Belgium, the Netherlands, Germany, southern North Sea). *Quaternary Science Reviews, 26*(25-28), 3249-3275.

Vermeersen, B. L., Slangen, A. B., Gerkema, T., Baart, F., Cohen, K. M., Dangendorf, S., ... & Van Der Wegen, M. (2018). Sea-level change in the Dutch Wadden Sea. *Netherlands Journal of Geosciences*, *97*(3), 79-127.